PERGAMON

International Journal of Solids and Structures 37 (2000) 899–918

INTERNATIONAL JOURNAL OF SOLIDS and STRUCTURES

www.elsevier.com/locate/ijsolstr

Development of special multi-material elements

Ai Kah Soh*

Department of Mechanical Engineering, The University of Hong Kong, Pokfulam Road, Hong Kong

Received 2 June 1998; in revised form 16 November 1998

Abstract

A procedure for developing multi-material elements, which are able to eliminate the weakness of the conventional finite elements in determining the stress distributions along the interfaces of different materials, has been proposed. The results obtained by this multi-material element type are in good agreement with those obtained by a modified finite element approach, which employs the least square fitting method to improve the calculation of interfacial stresses. Moreover, these two solutions are superior to the conventional finite element solution. The improvements made by these two modified solutions are entirely due to the imposition of the necessary and sufficient equilibrium and compatibility conditions at the interfaces. It is worth noting that while the two modified finite element approaches provide comparable accuracy, the proposed approach using new multi-material elements is much easier to implement.

Keywords: Multi-material; Bi- and tri-materials; Interfacial stresses; Finite elements; Least square method; Fibre–matrix interface

1. Introduction

Soh (1993a) has illustrated the weakness of the conventional finite element procedure in determining the stress distribution along a perfectly bonded fibre–matrix interface. The said weakness was due to the fact that the chosen element displacement functions do not explicitly and/or implicitly satisfy the equilibrium and compatibility conditions that prevail at an interface. As a result, the interfacial stresses obtained from the matrix and fibre elements having a common interface are incompatible. This is especially marked in the vicinity of geometric stress concentrations, since the stresses along the interfaces can only be determined by extrapolation or some arbitrary means of averaging.

Soh (1993a) has proposed a procedure to eliminate the above-mentioned weakness by employing the method of least square fitting. However, the said procedure is tedious because it involves the

* Tel.: +852-2858-5415; fax: +852-2858-5415.
E-mail address: aksoh@hkucc.hku.hk (A.K. Soh)

0020-7683/00/$ - see front matter
PII: S0020-7683(99)00064-5

Nomenclature

E	Modulus of elasticity
G	Modulus of rigidity
r, θ, z	Cylindrical coordinates
x, y, z	Cartesian coordinates
u, v, w	Displacement components
ξ, η, ζ	Isoparametric coordinates
ν	Poisson's ratio
$\bar{\sigma}$	Average axial stress
$\sigma_r, \sigma_\theta, \sigma_z$	Normal stresses parallel to r, θ and z axes, respectively
$\sigma_x, \sigma_y, \sigma_z$	Normal stresses parallel to x, y and z axes, respectively
$\sigma_\xi, \sigma_\eta, \sigma_\zeta$	Normal stresses parallel to ξ, η and ζ axes, respectively
$\tau_{r\theta}, \tau_{\theta z}, \tau_{zr}$	Shear stresses in r, θ, z coordinates
$\tau_{xy}, \tau_{yz}, \tau_{zx}$	Shear stresses in x, y, z coordinates
$\tau_{\xi\eta}, \tau_{\eta\zeta}, \tau_{\zeta\xi}$	Shear stresses in ξ, η and ζ coordinates

employment of high order polynomials for least square fitting after the determination of all nodal displacements by the conventional finite element method. This is especially so in the case of three-dimensional analysis because the procedure of least square fitting has to be carried out twice in order to determine all the stress and strain components at any nodal point considered.

The problem of accurate prediction of interfacial stresses is also a major concern for researchers working on composite laminates (Noor and Burton, 1990). Two fundamental approaches have been adopted by researchers to solve the said problem. In the first approach, a multilayered plate/shell is substituted by an equivalent, anisotropic, single layer plate/shell and a power-series expansion is assumed for the displacement field in terms of the thicknesswise coordinate (Librescu and Khdeir, 1988). Efforts have also been made by some researchers to modify a three-dimensional element to a two-dimensional one for the analysis of laminated composite plates/shells (Buragohain and Ravichandran, 1994). In the second approach, the conditions of continuity of interlaminar stresses in a multilayered plate/shell are satisfied by introducing generalized displacements at the layer level and imposed contact conditions as constraints on each layer. This approach was adopted by Murakami (1986), Reddy (1989) and Di Sciuva (1995) to develop multilayered plate elements.

In this paper, new multi-material three-dimensional elements will be developed to eliminate the weakness of the conventional finite element method. The development procedure and potential accuracy of this multi-material element type can be illustrated by considering the behaviour of two composite models, each with a discontinuous fibre, subjected to prescribed loads. These two models were devised based on an idealised three-dimensional model, which has a discontinuous fibre in the centre, as shown in Fig. 1.

2. Procedure for development of multi-material elements

Fig. 2 shows a three-dimensional brick element which consists of several materials of different mechanical properties. The displacement fields in this multi-material element can be expressed as

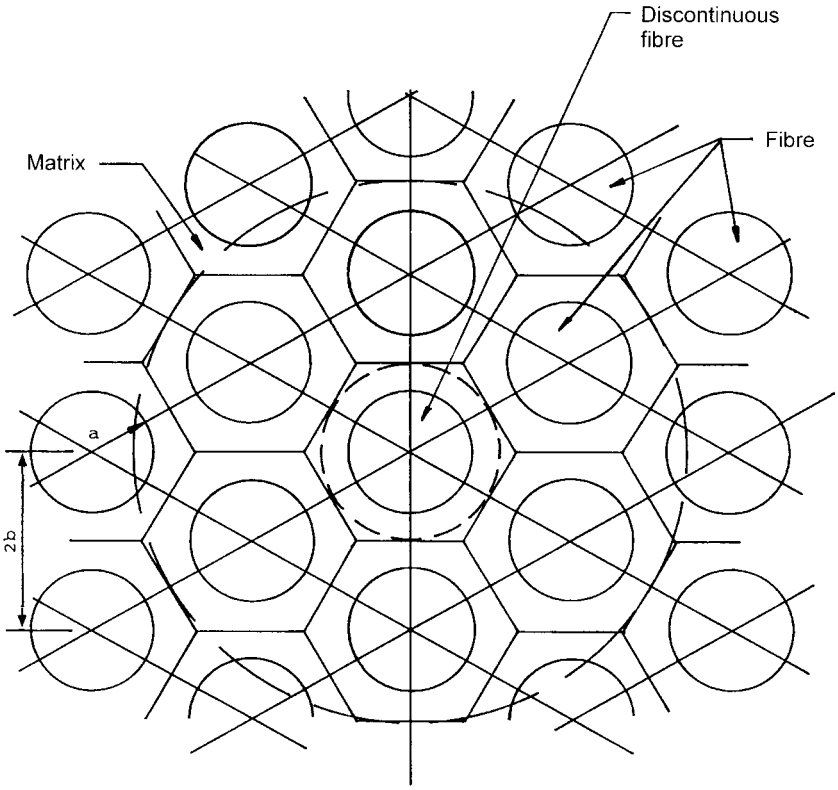

Fig. 1. An idealised three-dimensional fibre-reinforced composite.

$$\left.\begin{array}{lll} u_{\mathrm{m}_1} = f_{\mathrm{m}_1}(\xi,\eta,\zeta); & v_{\mathrm{m}_1} = g_{\mathrm{m}_1}(\xi,\eta,\zeta); & w_{\mathrm{m}_1} = h_{\mathrm{m}_1}(\xi,\eta,\zeta) \\ & \vdots & \\ u_{\mathrm{m}_s} = f_{\mathrm{m}_s}(\xi,\eta,\zeta); & v_{\mathrm{m}_s} = g_{\mathrm{m}_s}(\xi,\eta,\zeta); & w_{\mathrm{m}_s} = h_{\mathrm{m}_s}(\xi,\eta,\zeta) \end{array}\right\}, \tag{1}$$

where u_{m_s}, v_{m_s} and w_{m_s} are the displacements of the s-th material in the ξ, η and ζ directions, respectively.

Assume that the interface between the i-th and $(i+1)$-th materials is at $\zeta=\zeta_i$, the conditions of equilibrium and compatibility to be satisfied at the interface are:

$$\left.\begin{array}{lll} u_{\mathrm{m}_i} = u_{\mathrm{m}_{i+1}}; & v_{\mathrm{m}_i} = v_{\mathrm{m}_{i+1}}; & w_{\mathrm{m}_i} = w_{\mathrm{m}_{i+1}} \\ (\sigma_\zeta)_{\mathrm{m}_i} = (\sigma_\zeta)_{\mathrm{m}_{i+1}}; & (\tau_{\zeta\xi})_{\mathrm{m}_i} = (\tau_{\zeta\xi})_{\mathrm{m}_{i+1}}; & (\tau_{\eta\zeta})_{\mathrm{m}_i} = (\tau_{\eta\zeta})_{\mathrm{m}_{i+1}} \end{array}\right\}, \text{ at } \zeta = \zeta_i. \tag{2}$$

By implementing the conditions of equilibrium and compatibility at all the interfaces between different materials, a set of equations will be obtained which enables the elimination of some coefficient from the displacement functions. Thus, the displacement fields in the multi-material element can be expressed, respectively, as

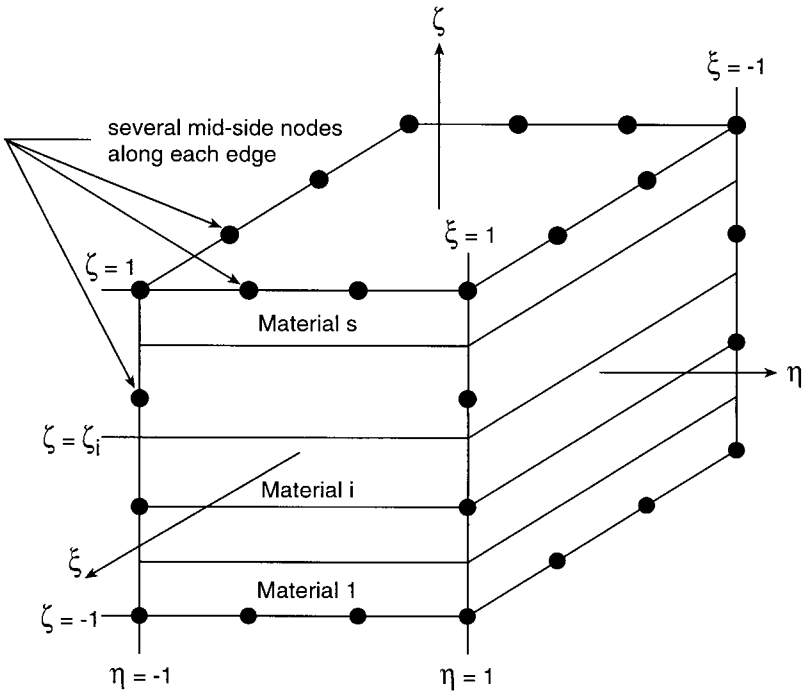

Fig. 2. A typical multi-material brick element.

$$\left.\begin{aligned}
&\{\boldsymbol{\delta}_{\mathrm{m}_1}\} = \{u_{\mathrm{m}_1}, v_{\mathrm{m}_1}, w_{\mathrm{m}_1}\}^T = [\boldsymbol{\Omega}_{\mathrm{m}_1}]\{\boldsymbol{\Lambda}\} \\
&\{\boldsymbol{\delta}_{\mathrm{m}_2}\} = \{u_{\mathrm{m}_2}, v_{\mathrm{m}_2}, w_{\mathrm{m}_2}\}^T = [\boldsymbol{\Omega}_{\mathrm{m}_2}]\{\boldsymbol{\Lambda}\} \\
&\vdots \\
&\{\boldsymbol{\delta}_{\mathrm{m}_s}\} = \{u_{\mathrm{m}_s}, v_{\mathrm{m}_s}, w_{\mathrm{m}_s}\}^T = [\boldsymbol{\Omega}_{\mathrm{m}_s}]\{\boldsymbol{\Lambda}\}
\end{aligned}\right\}, \tag{3}$$

where $\{\boldsymbol{\Lambda}\}$ consists of all the independent coefficients of the displacement functions; and $[\boldsymbol{\Omega}_{\mathrm{m}_1}], [\boldsymbol{\Omega}_{\mathrm{m}_2}], \ldots, [\boldsymbol{\Omega}_{\mathrm{m}_s}]$ consist of powers and products of ξ, η and ζ.

By substituting the coordinates and displacements of each and every node in the region of the first material, including those nodes at the interface between the first and second materials (if there are such nodes), into the first part of Eq. (3), we obtain

$$\left\{\boldsymbol{\delta}^e_{\mathrm{m}_1}\right\} = [\boldsymbol{\Omega}_{\mathrm{c}_1}]\{\boldsymbol{\Lambda}\}, \tag{4}$$

where $\{\boldsymbol{\delta}^e_{\mathrm{m}_1}\}$ is the displacement vector of those nodes, including interfacial nodes, in the first material; and $[\boldsymbol{\Omega}_{\mathrm{c}_1}]$ is a coefficient matrix consisting of powers and products of ξ, η and ζ.

By employing the same procedure for the rest of the materials, we obtain

$$\left.\begin{aligned}
&\left\{\boldsymbol{\delta}^e_{\mathrm{m}_2}\right\} = [\boldsymbol{\Omega}_{\mathrm{c}_2}]\{\boldsymbol{\Lambda}\} \\
&\vdots \\
&\left\{\boldsymbol{\delta}^e_{\mathrm{m}_s}\right\} = [\boldsymbol{\Omega}_{\mathrm{c}_s}]\{\boldsymbol{\Lambda}\}
\end{aligned}\right\}. \tag{5}$$

Note that no interfacial nodes are involved in the last part of Eq. (5).

By combining Eqs. (4) and (5), we obtain

$$\{\boldsymbol{\delta}^e\} = [\boldsymbol{\Omega}_c]\{\boldsymbol{\Lambda}\}, \tag{6}$$

where

$$\{\boldsymbol{\delta}^e\}^T = \left\{\{\boldsymbol{\delta}^e_{m_1}\}^T, \{\boldsymbol{\delta}^e_{m_2}\}^T, \ldots, \{\boldsymbol{\delta}^e_{m_s}\}^T\right\}$$

and

$$[\boldsymbol{\Omega}_c]^T = \left[\boldsymbol{\Omega}^T_{c_1}, \boldsymbol{\Omega}^T_{c_2}, \ldots, \boldsymbol{\Omega}^T_{c_s}\right].$$

Eq. (6) can be expressed as

$$\{\boldsymbol{\Lambda}\} = [\boldsymbol{\Omega}_c]^{-1}\{\boldsymbol{\delta}^e\}. \tag{7}$$

The displacement fields at any point within the i-th material of the element can be expressed in terms of the nodal displacement vector as follows:

$$\{\boldsymbol{\delta}_{m_i}\} = [\boldsymbol{\Omega}_{m_i}][\boldsymbol{\Omega}_c]^{-1}\{\boldsymbol{\delta}^e\}. \tag{8}$$

By analogy with the traditional finite element method (Bathe, 1996), the term $[\boldsymbol{\Omega}_{m_i}][\boldsymbol{\Omega}_c]^{-1}$ represents the shape functions of the i-th region of the element. Accordingly, by adopting standard finite element formulations, we can easily obtain the strain vector, $\{\boldsymbol{\varepsilon}\}^T = \{\varepsilon_\xi, \varepsilon_\eta, \varepsilon_\zeta, \gamma_{\xi\eta}, \gamma_{\eta\zeta}, \gamma_{\zeta\xi}\}^T$, at any point in the i-th material of the element in terms of the nodal displacement vector, i.e.,

$$\{\boldsymbol{\varepsilon}_{m_i}\} = [\mathbf{S}]\{\boldsymbol{\delta}_{m_i}\} = [\mathbf{S}][\boldsymbol{\Omega}_{m_i}][\boldsymbol{\Omega}_c]^{-1}\{\boldsymbol{\delta}^e\} = [\mathbf{B}_{m_i}]\{\boldsymbol{\delta}^e\}. \tag{9}$$

where

$$[\mathbf{S}] = \begin{bmatrix} \partial/\partial\xi & 0 & 0 \\ 0 & \partial/\partial\eta & 0 \\ 0 & 0 & \partial/\partial\zeta \\ \partial/\partial\eta & \partial/\partial\xi & 0 \\ 0 & \partial/\partial\zeta & \partial/\partial\eta \\ \partial/\partial\zeta & 0 & \partial/\partial\xi \end{bmatrix}$$

and

$$[\mathbf{B}_{m_i}] = [\mathbf{S}][\boldsymbol{\Omega}_{m_i}][\boldsymbol{\Omega}_c]^{-1}.$$

The element stiffness matrix is given by

$$[\mathbf{K}^e] = \int_{-1}^{1}\int_{-1}^{1}\int_{-1}^{1} [\mathbf{B}]^T[\mathbf{D}][\mathbf{B}]\det[\mathbf{J}]\mathrm{d}\xi\,\mathrm{d}\eta\,\mathrm{d}\zeta = \sum_{i=1}^{i=s}\int\int\int_{V_{m_i}} [\mathbf{B}_{m_i}]^T[\mathbf{D}_{m_i}][\mathbf{B}_{m_i}]\det[\mathbf{J}]\mathrm{d}\xi\,\mathrm{d}\eta\,\mathrm{d}\zeta, \tag{10}$$

where

$[\mathbf{D}_{m_i}]$ is the elasticity matrix for the i-th region of the element,
$\det[\mathbf{J}]$ is the determinant of the Jacobian matrix, and
V_{m_i} is the volume of the i-th region.

These type of elements can be employed together with other types of elements to improve the accuracy of the stresses computed at the interfaces between different materials.

3. Development of a twenty-noded three-dimensional brick element

The displacement fields in matrix and fibre regions of the twenty-noded bi-material element, as shown in Fig. 3, are, respectively, given by

$$\{\boldsymbol{\delta}_{\mathrm{m}}\} = \begin{Bmatrix} u_{\mathrm{m}} \\ v_{\mathrm{m}} \\ w_{\mathrm{m}} \end{Bmatrix} = \begin{Bmatrix} g_{\mathrm{m}_1}(\xi,\eta,\zeta) \\ g_{\mathrm{m}_2}(\xi,\eta,\zeta) \\ g_{\mathrm{m}_3}(\xi,\eta,\zeta) \end{Bmatrix}$$

and

$$\{\boldsymbol{\delta}\}_{\mathrm{f}} = \begin{Bmatrix} u_{\mathrm{f}} \\ v_{\mathrm{f}} \\ w_{\mathrm{f}} \end{Bmatrix} = \begin{Bmatrix} g_{\mathrm{f}_1}(\xi,\eta,\zeta) \\ g_{\mathrm{f}_2}(\xi,\eta,\zeta) \\ g_{\mathrm{f}_3}(\xi,\eta,\zeta) \end{Bmatrix}, \tag{11}$$

where

$$g_{\mathrm{m}_i} = \alpha_{i,1} + \alpha_{i,2}\xi + \alpha_{i,3}\eta + \alpha_{i,4}\zeta + \alpha_{i,5}\xi^2 + \alpha_{i,6}\xi\eta + \alpha_{i,7}\eta^2 + \alpha_{i,8}\eta\zeta + \alpha_{i,9}\zeta^2 + \alpha_{i,10}\xi\zeta + \alpha_{i,11}\xi^2\eta + \alpha_{i,12}\xi\eta^2 + \alpha_{i,13}\eta^2\zeta + \alpha_{i,14}\eta\zeta^2 + \alpha_{i,15}\zeta^2\xi + \alpha_{i,16}\zeta\xi^2 + \alpha_{i,17}\xi\eta\zeta$$

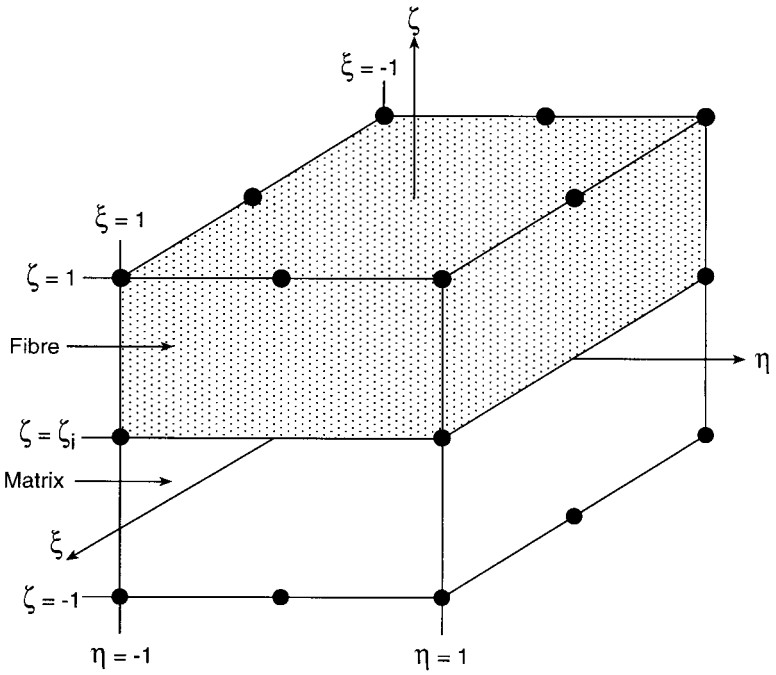

Fig. 3. A typical bi-material brick element.

and

$$g_{fi} = \beta_{i,1} + \beta_{i,2}\xi + \beta_{i,3}\eta + \beta_{i,4}\zeta + \beta_{i,5}\xi^2 + \beta_{i,6}\xi\eta + \beta_{i,7}\eta^2 + \beta_{i,8}\eta\zeta + \beta_{i,9}\zeta^2 + \beta_{i,10}\xi\zeta + \beta_{i,11}\xi^2\eta + \beta_{i,12}\xi\eta^2 + \beta_{i,13}\eta^2\zeta + \beta_{i,14}\eta\zeta^2 + \beta_{i,15}\zeta^2\xi + \beta_{i,16}\zeta\xi^2 + \beta_{i,17}\xi\eta\zeta,$$

in which $\alpha_{i,1}$, $\alpha_{i,2}$,..., $\alpha_{i,17}$ and $\beta_{i,1}$, $\beta_{i,2}$,..., $\beta_{i,17}$ are arbitrary constants and $i = 1$, 2 and 3.

The conditions of equilibrium and compatibility to be satisfied at the interface are:

$$\left.\begin{array}{lll} u_{\mathrm{m}} = u_{\mathrm{f}}; & v_{\mathrm{m}} = v_{\mathrm{f}}; & w_{\mathrm{m}} = w_{\mathrm{f}} \\ (\sigma_\zeta)_{\mathrm{m}} = (\sigma_\zeta)_{\mathrm{f}}; & (\tau_{\zeta\xi})_{\mathrm{m}} = (\tau_{\zeta\xi})_{\mathrm{f}}; & (\tau_{\zeta\eta})_{\mathrm{m}} = (\tau_{\zeta\eta})_{\mathrm{f}} \end{array}\right\} \text{ at } \zeta = 0, \tag{12}$$

where

$$\left.\begin{array}{l} (\sigma_\zeta)_k = \dfrac{E_k}{(1+\nu_k)(1-2\nu_k)} \quad \left((1-\nu_k)\dfrac{\partial w_k}{\partial \zeta} + \nu_k\dfrac{\partial u_k}{\partial \xi} + \nu_k\dfrac{\partial v_k}{\partial \eta}\right) \\ (\tau_{\zeta\xi})_k = G_k\left(\dfrac{\partial w_k}{\partial \xi} + \dfrac{\partial u_k}{\partial \zeta}\right) \\ (\tau_{\zeta\eta})_k = G_k\left(\dfrac{\partial w_k}{\partial \eta} + \dfrac{\partial v_k}{\partial \zeta}\right) \end{array}\right\}; \; k = \mathrm{m,f}. \tag{13}$$

Note that E_k, G_k and ν_k are the moduli of elasticity and rigidity and Poisson's ratio of the material, respectively.

By implementing the conditions of equilibrium and compatibility, we obtain

$$\beta_{1,1} = \alpha_{1,1};\ \beta_{1,2} = \alpha_{1,2};\ \beta_{1,3} = \alpha_{1,3};\ \beta_{1,5} = \alpha_{1,5},$$

$$\beta_{1,6} = \alpha_{1,6};\ \beta_{1,7} = \alpha_{1,7};\ \beta_{1,11} = \alpha_{1,11};\ \beta_{1,12} = \alpha_{1,12},$$

$$\beta_{2,1} = \alpha_{2,1};\ \beta_{2,2} = \alpha_{2,2};\ \beta_{2,3} = \alpha_{2,3};\ \beta_{2,5} = \alpha_{2,5},$$

$$\beta_{2,6} = \alpha_{2,6};\ \beta_{2,7} = \alpha_{2,7};\ \beta_{2,11} = \alpha_{2,11};\ \beta_{2,12} = \alpha_{2,12},$$

$$\beta_{3,1} = \alpha_{3,1};\ \beta_{3,2} = \alpha_{3,2};\ \beta_{3,3} = \alpha_{3,3};\ \beta_{3,5} = \alpha_{3,5},$$

$$\beta_{3,6} = \alpha_{3,6};\ \beta_{3,7} = \alpha_{3,7};\ \beta_{3,11} = \alpha_{3,11};\ \beta_{3,12} = \alpha_{3,12},$$

$$\beta_{1,4} = \Gamma_2\alpha_{1,4} + (\Gamma_2 - 1)\alpha_{3,12},$$

$$\beta_{1,8} = \Gamma_2\alpha_{1,8} + (\Gamma_2 - 1)\alpha_{3,6},$$

$$\beta_{1,10} = \Gamma_2\alpha_{1,10} + 2(\Gamma_2 - 1)\alpha_{3,5},$$

$$\beta_{1,13} = \Gamma_2\alpha_{1,13} + (\Gamma_2 - 1)\alpha_{3,12},$$

$$\beta_{1,16} = \Gamma_2\alpha_{1,16},$$

$$\beta_{1,17} = \Gamma_2\alpha_{1,17} + 2(\Gamma_2 - 1)\alpha_{3,11},$$

$$\beta_{2,4} = \Gamma_2\alpha_{2,4} + (\Gamma_2 - 1)\alpha_{3,3},$$

$$\beta_{2,8} = \Gamma_2\alpha_{2,8} + 2(\Gamma_2 - 1)\alpha_{3,7},$$

$$\beta_{2,10} = \Gamma_2\alpha_{2,10} + (\Gamma_2 - 1)\alpha_{3,6},$$

$$\beta_{2,13} = \Gamma_2\alpha_{2,13},$$

$$\beta_{2,16} = \Gamma_2\alpha_{2,16} + (\Gamma_2 - 1)\alpha_{3,11},$$

$$\beta_{2,17} = \Gamma_2\alpha_{2,17} + 2(\Gamma_2 - 1)\alpha_{3,12},$$

$$\beta_{3,4} = \frac{[\Gamma_1(1 - v_m)\alpha_{3,4} + (\Gamma_1 v_m - v_f)(\alpha_{1,2} + \alpha_{2,3})]}{(1 - v_f)},$$

$$\beta_{3,8} = \frac{[\Gamma_1(1 - v_m)\alpha_{3,8} + (\Gamma_1 v_m - v_f)(\alpha_{1,6} + 2\alpha_{2,7})]}{(1 - v_f)},$$

$$\beta_{3,10} = \frac{[\Gamma_1(1 - v_m)\alpha_{3,10} + (\Gamma_1 v_m - v_f)(2\alpha_{1,5} + \alpha_{2,6})]}{(1 - v_f)},$$

$$\beta_{3,13} = \frac{[\Gamma_1(1 - v_m)\alpha_{3,13} + (\Gamma_1 v_m - v_f)\alpha_{1,12}]}{(1 - v_f)},$$

$$\beta_{3,16} = \frac{[\Gamma_1(1 - v_m)\alpha_{3,16} + (\Gamma_1 v_m - v_f)\alpha_{2,11}]}{(1 - v_f)},$$

$$\beta_{3,17} = \frac{[\Gamma_1(1 - v_m)\alpha_{3,17} + 2(\Gamma_1 v_m - v_f)(\alpha_{1,11} + \alpha_{2,12})]}{(1 - v_f)},$$

where

$$\Gamma_1 = \frac{E_m}{E_f}\left[\frac{(1 + v_f)(1 - 2v_f)}{(1 + v_m)(1 - 2v_m)}\right]$$

and

$$\Gamma_2 = \frac{G_m}{G_f}.$$

Thus, the displacement fields in the fibre region of the bi-material element can be expressed as

$$u_f = \alpha_{1,1} + \alpha_{1,2}\xi + \alpha_{1,3}\eta + [\Gamma_2\alpha_{1,4} + (\Gamma_2 - 1)\alpha_{3,12}]\zeta + \alpha_{1,5}\xi^2 + \alpha_{1,6}\xi\eta + \alpha_{1,7}\eta^2 + [\Gamma_2\alpha_{1,8} + (\Gamma_2 - 1)\alpha_{3,6}]\eta\zeta + \beta_{1,9}\zeta^2 + [\Gamma_2\alpha_{1,10} + 2(\Gamma_2 - 1)\alpha_{3,5}]\xi\zeta + \alpha_{1,11}\xi^2\eta + \alpha_{1,12}\xi\eta^2 + [\Gamma_2\alpha_{1,13} + (\Gamma_2 - 1)\alpha_{3,12}]\eta^2\zeta + \beta_{1,14}\eta\zeta^2 + \beta_{1,15}\zeta^2\xi + \Gamma_2\alpha_{1,16}\zeta\xi^2 + [\Gamma_2\alpha_{1,17} + 2(\Gamma_2 - 1)\alpha_{3,11}]\xi\eta\zeta, \tag{14}$$

$$v_f = \alpha_{2,1} + \alpha_{2,2}\xi + \alpha_{2,3}\eta + [\Gamma_2\alpha_{2,4} + (\Gamma_2 - 1)\alpha_{3,3}]\zeta + \alpha_{2,5}\xi^2 + \alpha_{2,6}\xi\eta + \alpha_{2,7}\eta^2 + [\Gamma_2\alpha_{2,8} + 2(\Gamma_2 - 1)\alpha_{3,7}]\eta\zeta + \beta_{2,9}\zeta^2 + [\Gamma_2\alpha_{2,10} + (\Gamma_2 - 1)\alpha_{3,6}]\xi\zeta + \alpha_{2,11}\xi^2\eta + \alpha_{2,12}\xi\eta^2 + \Gamma_2\alpha_{2,13}\eta^2\zeta + \beta_{2,14}\eta\zeta^2 + \beta_{2,15}\zeta^2\xi + [\Gamma_2\alpha_{2,16} + (\Gamma_2 - 1)\alpha_{3,11}]\zeta\xi^2 + [\Gamma_2\alpha_{2,17} + 2(\Gamma_2 - 1)\alpha_{3,12}]\xi\eta\zeta, \tag{15}$$

$$w_f = \alpha_{3,1} + \alpha_{3,2}\xi + \alpha_{3,3}\eta + \frac{1}{(1 - v_f)}[\Gamma_2(1 - v_m)\alpha_{3,4} + (\Gamma_1 v_m - v_f)(\alpha_{1,2} + \alpha_{2,3})]\zeta + \alpha_{3,5}\xi^2 + \alpha_{3,6}\xi\eta + \alpha_{3,7}\eta^2 + \frac{1}{(1 - v_f)}[\Gamma_1(1 - v_m)\alpha_{3,8} + (\Gamma_1 v_m - v_f)(\alpha_{1,6} + 2\alpha_{2,7})]\eta\zeta + \beta_{3,9}\zeta^2 + \frac{1}{(1 - v_f)}[\Gamma_1(1 - v_m)\alpha_{3,10} + (\Gamma_1 v_m - v_f)(2\alpha_{1,5} + \alpha_{2,6})]\xi\zeta + \alpha_{3,11}\xi^2\eta + \alpha_{3,12}\xi\eta^2 + \frac{1}{(1 - v_f)}[\Gamma_1(1 - v_m)\alpha_{3,13} + (\Gamma_1 v_m - v_f)\alpha_{1,12}]\eta^2\zeta + \beta_{3,14}\eta\zeta^2 + \beta_{3,15}\zeta^2\xi + \frac{1}{(1 - v_f)}[\Gamma_1(1 - v_m)\alpha_{3,16} + (\Gamma_1 v_m - v_f)\alpha_{2,11}]\zeta\xi^2 + \frac{1}{(1 - v_f)}[\Gamma_1(1 - v_m)\alpha_{3,17} + 2(\Gamma_1 v_m - v_f)(\alpha_{1,11} + \alpha_{2,12})]\xi\eta\zeta. \tag{16}$$

The above equations can be expressed as

$$\{\boldsymbol{\delta}_m\} = [\boldsymbol{\Omega}_m]\{\boldsymbol{\Lambda}\} \tag{17}$$

and

$$\{\boldsymbol{\delta}_f\} = [\boldsymbol{\Omega}_f]\{\boldsymbol{\Lambda}\}, \tag{18}$$

where

$$\{\boldsymbol{\delta}_m\} = \{u_m, v_m, w_m\}^T,$$

$$\{\boldsymbol{\delta}_f\} = \{u_f, v_f, w_f\}^T,$$

$$[\boldsymbol{\Omega}_m] = \begin{bmatrix} \boldsymbol{\Omega}_{\xi m} \\ \boldsymbol{\Omega}_{\eta m} \\ \boldsymbol{\Omega}_{\zeta m} \end{bmatrix},$$

$$[\mathbf{\Omega}_{\mathrm{f}}] = \begin{bmatrix} \mathbf{\Omega}_{\xi\mathrm{f}} \\ \mathbf{\Omega}_{\eta\mathrm{f}} \\ \mathbf{\Omega}_{\zeta\mathrm{f}} \end{bmatrix}$$

and

$$\{\mathbf{\Lambda}\} = \{\alpha_{1,1},\alpha_{1,2},\ldots,\alpha_{1,17},\alpha_{2,1},\alpha_{2,2},\ldots,\alpha_{2,17},\alpha_{3,1},\alpha_{3,2}$$

$$,\ldots,\alpha_{3,17},\beta_{1,9},\beta_{1,14},\beta_{1,15},\beta_{2,9},\beta_{2,14},\beta_{2,15},\beta_{3,9},\beta_{3,14},\beta_{3,15}\}^T$$

Note that $[\mathbf{\Omega}_{\xi\mathrm{m}}]$, $[\mathbf{\Omega}_{\eta\mathrm{m}}]$ and $[\mathbf{\Omega}_{\zeta\mathrm{m}}]$ are row matrices consisting of powers and products of ξ, η and ζ for the displacements in the ξ, η and ζ directions, respectively, in the matrix region. $[\mathbf{\Omega}_{\xi\mathrm{f}}]$, $[\mathbf{\Omega}_{\eta\mathrm{f}}]$ and $[\mathbf{\Omega}_{\zeta\mathrm{f}}]$ are the corresponding row matrices in the fibre region.

If Eqs. (17) and (18) are satisfied at nodes 1 through 12 and nodes 13 through 20, respectively, we obtain

$$\{\boldsymbol{\delta}^e\} = [\mathbf{\Omega}_{\mathrm{c}}]\{\mathbf{\Lambda}\}, \tag{19}$$

where

$$\{\boldsymbol{\delta}^e\} = \left\{u_{\mathrm{m}}^1,v_{\mathrm{m}}^1,w_{\mathrm{m}}^1,u_{\mathrm{m}}^2,v_{\mathrm{m}}^2,w_{\mathrm{m}}^2,\ldots,u_{\mathrm{m}}^{12},v_{\mathrm{m}}^{12},w_{\mathrm{m}}^{12},u_{\mathrm{f}}^{13},v_{\mathrm{f}}^{13},w_{\mathrm{f}}^{13},u_{\mathrm{f}}^{14},v_{\mathrm{f}}^{14},w_{\mathrm{f}}^{14},\ldots,u_{\mathrm{f}}^{20},v_{\mathrm{f}}^{20},w_{\mathrm{f}}^{20}\right\}$$

$$= \text{the nodal displacement vector.}$$

and

$$\{\mathbf{\Omega}_{\mathrm{c}}\}^T = \left\{\mathbf{\Omega}_{\xi\mathrm{m}^1}^T,\mathbf{\Omega}_{\eta\mathrm{m}^1}^T,\mathbf{\Omega}_{\zeta\mathrm{m}^1}^T,\ldots,\mathbf{\Omega}_{\xi\mathrm{m}^{12}}^T,\mathbf{\Omega}_{\eta\mathrm{m}^{12}}^T,\mathbf{\Omega}_{\zeta\mathrm{m}^{12}}^T,\mathbf{\Omega}_{\xi\mathrm{f}^{13}}^T,\mathbf{\Omega}_{\eta\mathrm{f}^{13}}^T,\mathbf{\Omega}_{\zeta\mathrm{f}^{13}}^T,\ldots,\mathbf{\Omega}_{\xi\mathrm{f}^{20}}^T,\mathbf{\Omega}_{\eta\mathrm{f}^{20}}^T,\mathbf{\Omega}_{\zeta\mathrm{f}^{20}}^T,\right\}.$$

Note that Eq. (19) is the same as Eq. (6) and the above-mentioned procedure can be employed to establish the element strain vector in terms of the nodal displacement vector, i.e.,

$$\left.\begin{array}{l} \{\boldsymbol{\varepsilon}_{\mathrm{m}}\} = [\mathbf{S}]\{\boldsymbol{\delta}_{\mathrm{m}}\} = [\mathbf{S}][\mathbf{\Omega}_{\mathrm{m}}][\mathbf{\Omega}_{\mathrm{c}}]^{-1}\{\boldsymbol{\delta}\}^e = [\mathbf{B}\mathrm{m}]\{\boldsymbol{\delta}\}^e \\ \{\boldsymbol{\varepsilon}_{\mathrm{f}}\} = [\mathbf{S}]\{\boldsymbol{\delta}_{\mathrm{f}}\} = [\mathbf{S}][\mathbf{\Omega}_{\mathrm{f}}][\mathbf{\Omega}_{\mathrm{c}}]^{-1}\{\boldsymbol{\delta}\}^e = [\mathbf{B}_{\mathrm{f}}]\{\boldsymbol{\delta}\}^e \end{array}\right\}, \tag{20}$$

where

$$[\mathbf{B}_{\mathrm{m}}] = [\mathbf{S}][\mathbf{\Omega}_{\mathrm{m}}][\mathbf{\Omega}_{\mathrm{c}}]^{-1}$$

and

$$[\mathbf{B}_{\mathrm{f}}] = [\mathbf{S}][\mathbf{\Omega}_{\mathrm{f}}][\mathbf{\Omega}_{\mathrm{c}}]^{-1}.$$

The element stiffness matrix is given by

$$[\mathbf{K}]^e = \int_{-1}^{1}\int_{-1}^{1}\int_{-1}^{1}[\mathbf{B}]^T[\mathbf{D}][\mathbf{B}]\det[\mathbf{J}]\mathrm{d}\xi\,\mathrm{d}\eta\,\mathrm{d}\zeta = \int\int\int_{V_{\mathrm{m}}}[\mathbf{B}_{\mathrm{m}}]^T[\mathbf{D}_{\mathrm{m}}][\mathbf{B}_{\mathrm{m}}]\det[\mathbf{J}]\mathrm{d}\xi\,\mathrm{d}\eta\,\mathrm{d}\zeta +$$

$$\int\int\int_{V_{\mathrm{f}}}[\mathbf{B}_{\mathrm{f}}]^T[\mathbf{D}_{\mathrm{f}}][\mathbf{B}_{\mathrm{f}}]\det[\mathbf{J}]\mathrm{d}\xi\,\mathrm{d}\eta\,\mathrm{d}\zeta, \tag{21}$$

where

$[\mathbf{D}_m]$, $[\mathbf{D}_f]$ are the elasticity matrices for the matrix and fibre regions, respectively; and V_m, V_f are the volumes of the matrix and fibre, respectively.

4. The least square method

Soh (1993a) has proposed a procedure to modify the conventional finite element method so as to allow the elastic stresses at the interface of a bi-material to be determined with improved accuracy. In the said proposal the traditional procedure (Zienkiewicz and Taylor, 1989) is used to determine all the nodal displacements without modification. Once the nodal displacements are obtained, the stresses at any nodal point lying on the fibre–matrix interface, as shown in Fig. 4, are determined by the following two-step procedure.

First, fit four continuous displacement functions, $(u_r)_m^f$, w_m^f, $(u_r)_f^f$ and w_f^f, by the least square method to those nodes that are lying in a constant θ-plane and surrounding/including the particular node considered, with the boundary conditions imposed to the five nodal points along the interface. Note that $(u_r)_m$ and $(u_r)_f$ are the displacements of the matrix and fibre in the r direction; and w_m and w_f are the corresponding displacements in the z direction.

By fitting the four displacement functions to the actual displacements of those nodes involved using the method of least squares, a set of 42 equations, each with an error term arising from the difference between the actual and best fitted displacements, can be obtained.

The interface boundary conditions are

$$(u_r)_m = (u_r)_f,$$

$$w_m = w_f,$$

$$(\sigma_r)_m = (\sigma_r)_f$$

and

$$(\tau_{rz})_m = (\tau_{rz})_f \tag{22}$$

By implementing the interface boundary conditions at the five nodes lying on the interface, another 20 equations are obtained. Note that each of these equations consists of an error term arising from the difference between the best-fitted values obtained from the fibre and matrix.

The 62 equations can be expressed in a matrix symbolic form, i.e.,

$$\{\boldsymbol{\delta}_0\} = [\boldsymbol{\Psi}_0]\{\boldsymbol{\Lambda}\} + \{\mathbf{I}\}, \tag{23}$$

where $\{\boldsymbol{\delta}_0\}$ is a column vector consisting of nodal displacements and zeros; $[\boldsymbol{\Psi}_0]$ is a coefficient matrix consisting of powers and products of r and z; $[\boldsymbol{\Lambda}]$ is a column vector consisting of the coefficients of the displacement functions for least square fitting; and $\{\mathbf{I}\}$ is a column vector consisting of the error terms.

By setting $\partial(\{\mathbf{I}\}^T\{\mathbf{I}\})/\partial\{\boldsymbol{\Lambda}\} = 0$ to satisfy the least square condition, we obtain

$$\{\boldsymbol{\Lambda}\} = \left([\boldsymbol{\Psi}_0]^T[\boldsymbol{\Psi}_0]\right)^{-1}[\boldsymbol{\Psi}_0]^T\boldsymbol{\delta}_0. \tag{24}$$

The best fitted displacement functions obtained can then be used to determine the stress components,

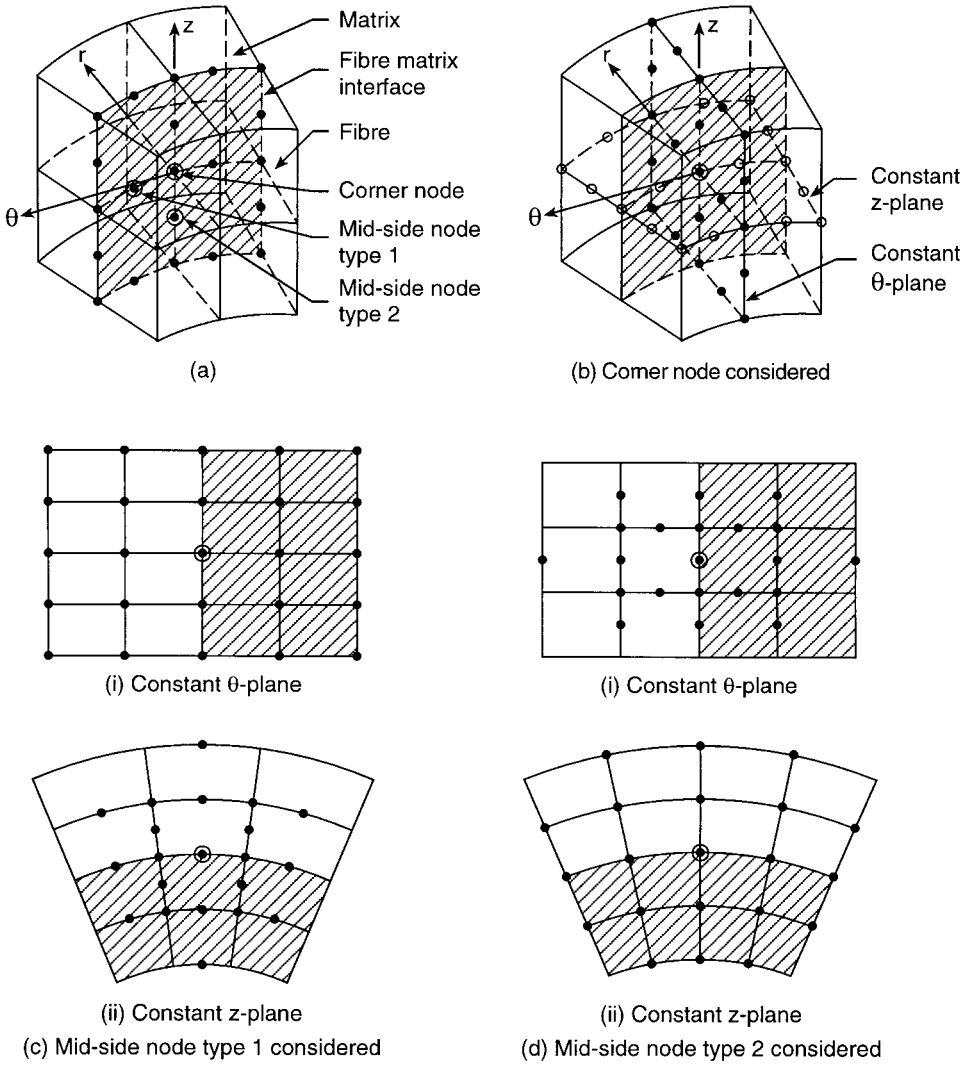

Fig. 4. Nodes involved in surface fitting for determining stresses at corner and mid-side nodes of a three-dimensional problem.

σ_r, σ_z and τ_{rz}, and the corresponding strain components at the nodes considered by employing the strain–displacement equations and stress–strain relations.

Second, fit four continuous displacement functions, $(u_r)^{\mathrm{f}}_{\mathrm{m}}$, $(v_\theta)^{\mathrm{f}}_{\mathrm{m}}$, $(u_r)^{\mathrm{f}}_{\mathrm{f}}$ and $(v_\theta)^{\mathrm{f}}_{\mathrm{f}}$, by the least square method to those nodes that are lying in a constant z-plane, surrounding/including the particular node considered, with the boundary conditions imposed to the five nodal points along the interface. Note that $(v_\theta)^{\mathrm{f}}_{\mathrm{m}}$ and $(v_\theta)^{\mathrm{f}}_{\mathrm{f}}$ are the tangential displacements of the fibre and matrix, respectively.

The interface boundary conditions are

$$(u_r)_{\mathrm{m}} = (u_r)_{\mathrm{f}},$$

$$(v_\theta)_{\mathrm{m}} = (v_\theta)_{\mathrm{f}},$$

$$(\sigma_r)_m = (\sigma_r)_f$$

and

$$(\tau_{r\theta})_m = (\tau_{r\theta})_f. \tag{25}$$

The best fitted displacement functions obtained can then be used to determine the stress components, σ_r, σ_θ and $\tau_{r\theta}$. Note that $\tau_{\theta z}$ cannot be directly obtained from the best fitted displacement functions because $\partial w/\partial\theta$ and $\partial v_\theta/\partial z$ are unknowns. However, the problem can be solved by employing the curve fitting technique to determine $\partial w/\partial\theta$ and $\partial v_\theta/\partial z$ at the nodal point of interest.

5. Finite element modeling

Two examples are employed to illustrate the versatility and potential accuracy of the proposed element type.

5.1. A discontinuous and some continuous fibres embedded in a matrix

Fig. 5 shows the three-dimensional model devised by considering only the cylindrical block, which consists of six continuous and one discontinuous fibres embedded in a matrix, of the idealised composite shown in Fig. 1. Because of the symmetry of the structure, it is sufficient to consider only a fraction of it and the mesh generated, as shown in Fig. 6, was employed to devise two finite element models. One model was built using solely the conventional isoparametric elements and the other using both the proposed bi-material and the conventional isoparametric element types. The elastic moduli of the fibre (duralumin) and matrix (Araldite CT200) were 760 and 32.5 MPa, respectively; and the corresponding Poisson's ratios were 0.28 and 0.38. The first model was employed to perform the conventional finite element analysis; and the nodal displacements obtained were used to perform least square fitting, as proposed by Soh (1993a), to determine the interfacial stresses with better accuracy. The second model was employed to illustrate the accuracy of the proposed bi-material element type.

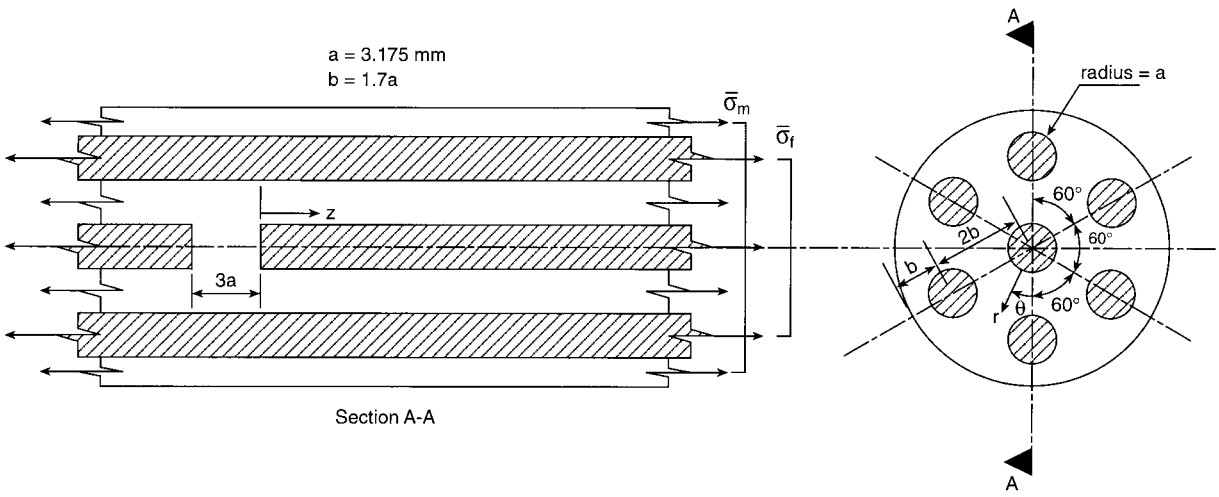

Fig. 5. Three-dimensional multifibre model subjected to tensile loads.

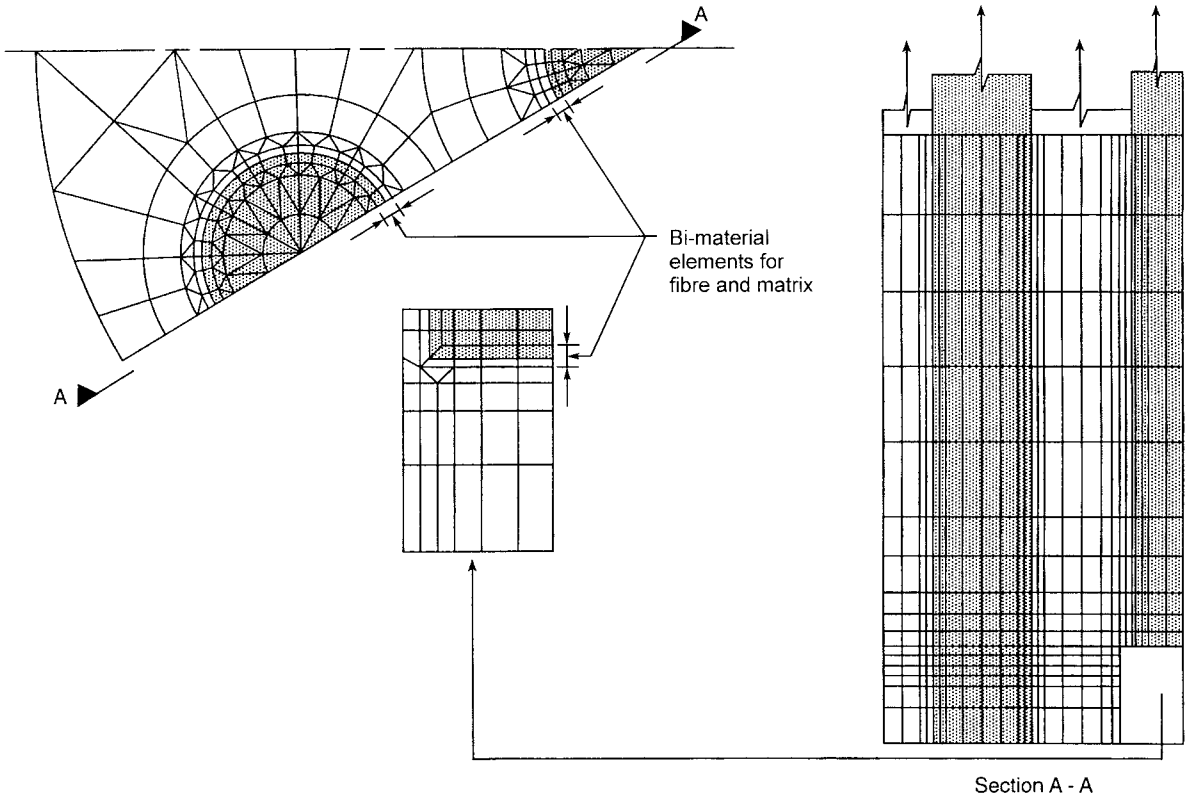

Fig. 6. Generation of two finite element models using: (i) the proposed bi-material and conventional isoparametric elements, and (ii) only the conventional isoparametric elements.

One of the commonly used conventional methods for determining the stress components at an interface nodal point is the graphical extrapolation method that uses the values of the stresses obtained for elements in the vicinity of the nodal point considered. This method has been clearly described by Soh (1993a) and, therefore, it will not be reiterated here.

5.2. A discontinuous fibre surrounded by matrix and composite layers

Fig. 7 shows an idealised model of the cylindrical block, which consists of six continuous and one discontinuous fibres embedded in a matrix, of the composite shown in Fig. 1. Note that the six continuous fibres and the surrounding matrix in a cylinder of inner and outer diameters 2b and 6b, respectively, have been replaced by a "simulated" composite layer. The elastic moduli of the fibre (E–glass) and matrix (epoxy resin) were 69.1714 and 3.4266 GPa, respectively; and the corresponding Poisson's ratios were 0.2 and 0.34. The "simulated" composite layer was transversely isotropic and the elastic constants (Soh, 1993b) were as follows:

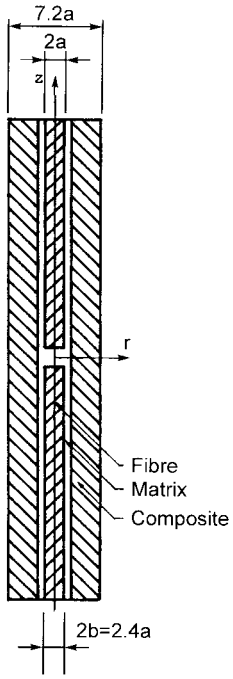

Fig. 7. An idealised composite model.

$$\begin{Bmatrix} \sigma_x \\ \sigma_y \\ \sigma_z \\ \tau_{xy} \\ \tau_{yz} \\ \tau_{zx} \end{Bmatrix} = \begin{bmatrix} 15.50 & 6.20 & 5.28 & 0 & 0 & 0 \\ 6.20 & 15.50 & 5.28 & 0 & 0 & 0 \\ 5.28 & 5.28 & 47.14 & 0 & 0 & 0 \\ 0 & 0 & 0 & 4.65 & 0 & 0 \\ 0 & 0 & 0 & 0 & 4.79 & 0 \\ 0 & 0 & 0 & 0 & 0 & 4.79 \end{bmatrix} \begin{Bmatrix} \varepsilon_x \\ \varepsilon_y \\ \varepsilon_z \\ \gamma_{xy} \\ \gamma_{yz} \\ \gamma_{zx} \end{Bmatrix} \text{(GPa)}$$

where σ_x, σ_y, σ_z, τ_{xy}, τ_{yz}, τ_{zx} and ε_x, ε_y, ε_z, γ_{xy}, γ_{yz}, γ_{zx} are the stress and strain components, respectively, in Cartesian coordinates.

The idealised model shown in Fig. 7 is, in fact, an axisymmetric model. However, a fraction of it was considered in order to carry out a three-dimensional analysis; and the mesh generated, as shown in Fig. 8, was employed to devise two finite element models. One model was built using solely the conventional isoparametric elements and the other using both the proposed and the conventional isoparametric element types. Similar to the first example, the nodal displacements, obtained from the analysis of the first model, were used to perform least square fitting to determine the interfacial stresses with better accuracy. In the case of the second model, bi- and tri-material elements were employed to model the fibre–matrix and fibre–matrix–composite interfaces, respectively. Note that the tri-material elements are also twenty-noded elements. The said model was devised to illustrate the accuracy of the proposed element type.

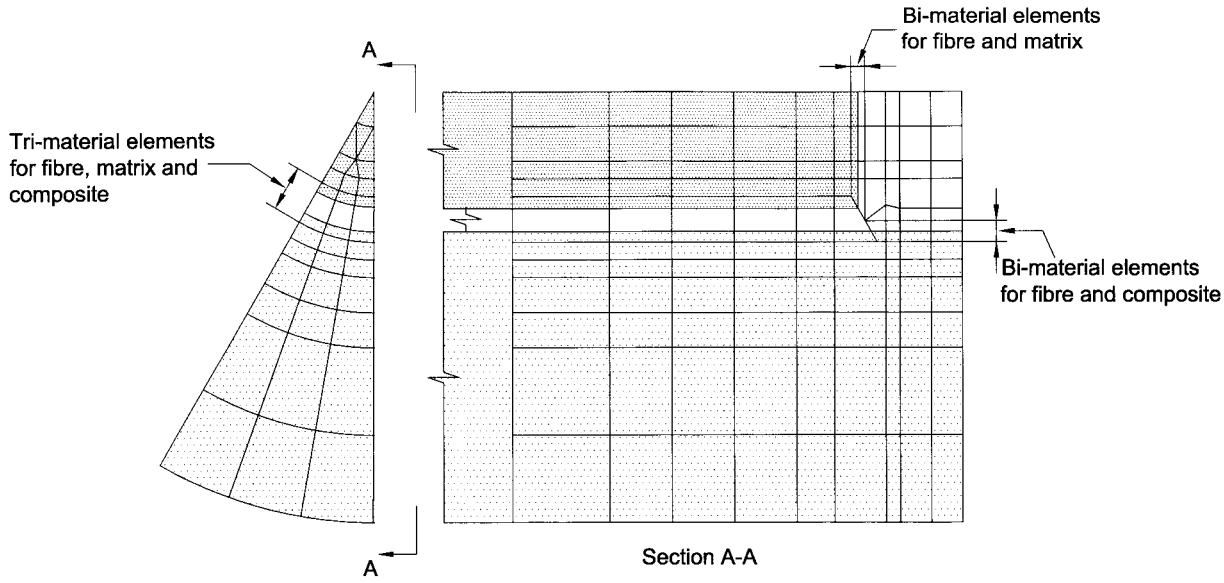

Fig. 8. Generation of two finite element models using: (i) the proposed multi-material and conventional isoparametric elements, and (ii) only the conventional isoparametric elements.

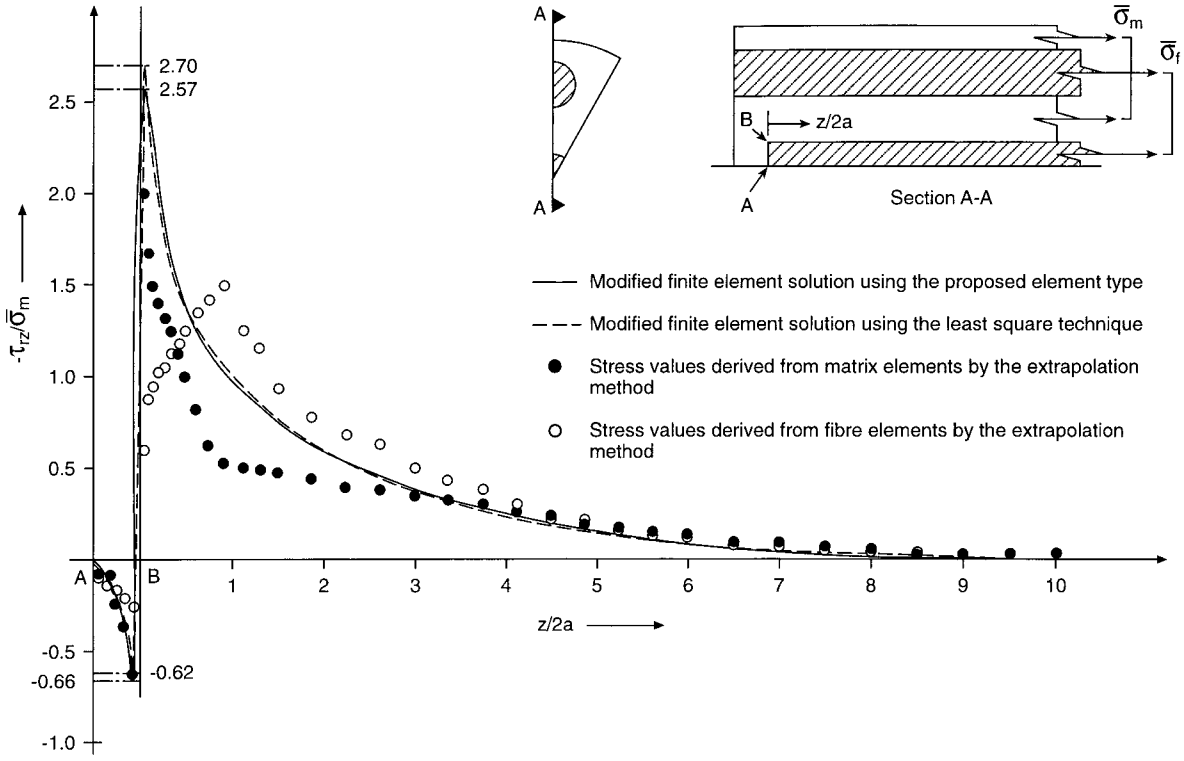

Fig. 9. Comparison of the interfacial shear stresses obtained by the modified and conventional finite element methods for a three-dimensional problem.

6. Discussion of results

6.1. A discontinuous and some continuous fibres embedded in a matrix

The interfacial shear stress distributions obtained by the two modified finite element solutions, one using the proposed bi-material element type and the other the least square fitting method, are compared with the conventional finite element solutions in Fig. 9. It is obvious that the stress values derived from the fibre and matrix elements are incompatible; the discrepancy between the maximum stresses is $0.5\bar{\sigma}_m$, where $\bar{\sigma}_m$ is the average axial stress in the matrix. Moreover, the maximum stresses determined from the fibre and matrix elements do not occur at the same position. Note that the stress values of the conventional solution can be estimated by averaging the values derived from the fibre and matrix elements.

The two modified finite element solutions are in better agreement as compared with the conventional finite element solution in terms of shape, maximum stress value, and position at which it occurs. The peak values of the ratio of interfacial shear stress to average axial stress in the matrix are 2.57, 2.70 and 1.30 for the modified finite element methods using bi-material elements and least square fitting, and the extrapolation method, respectively.

The interfacial lateral stress distributions, shown in Fig. 10, again show that the two modified finite element results are in good agreement and they are superior to the conventional results.

Fig. 11 shows the variations of the maximum interfacial shear stress and maximum interfacial tension with the end gap spacing, obtained by the two modified finite element solutions. It is obvious that these two solutions are in good agreement.

The improvements made by the use of the modified element type and analysis procedure are entirely

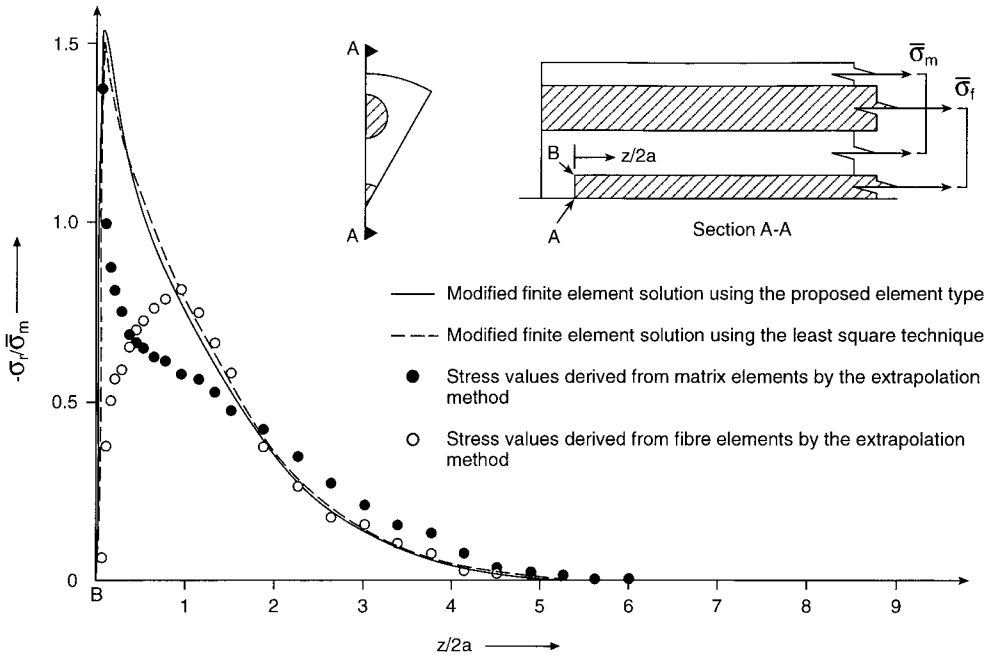

Fig. 10. Comparison of the interfacial lateral stresses obtained by the modified and conventional finite element methods for a three-dimensional problem.

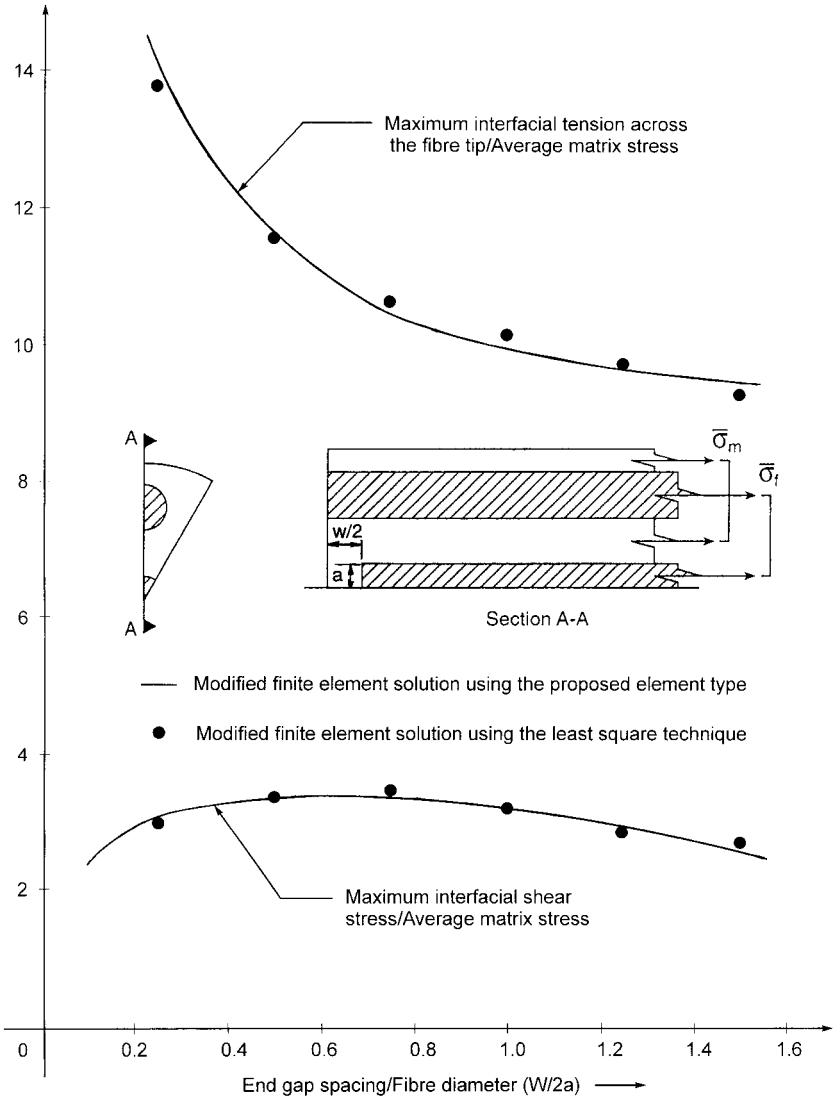

Fig. 11. Comparison of the results obtained by the proposed element type and the least square technique.

due to the imposition of the necessary and sufficient equilibrium and compatibility conditions at the fibre–matrix interface. This can be clearly seen from the magnitude of the discrepancy between the stress values derived from the fibre and matrix elements in the case of the conventional finite element analysis (refer to Figs. 9 and 10).

6.2. A discontinuous fibre surrounded by matrix and composite layers

Fig. 12 shows the interfacial shear stress distributions, along the fibre–matrix and matrix–composite interfaces, obtained by the two modified finite element solutions, one using the proposed multi-material element type and the other the least square fitting method. It is obvious that the two solutions agree

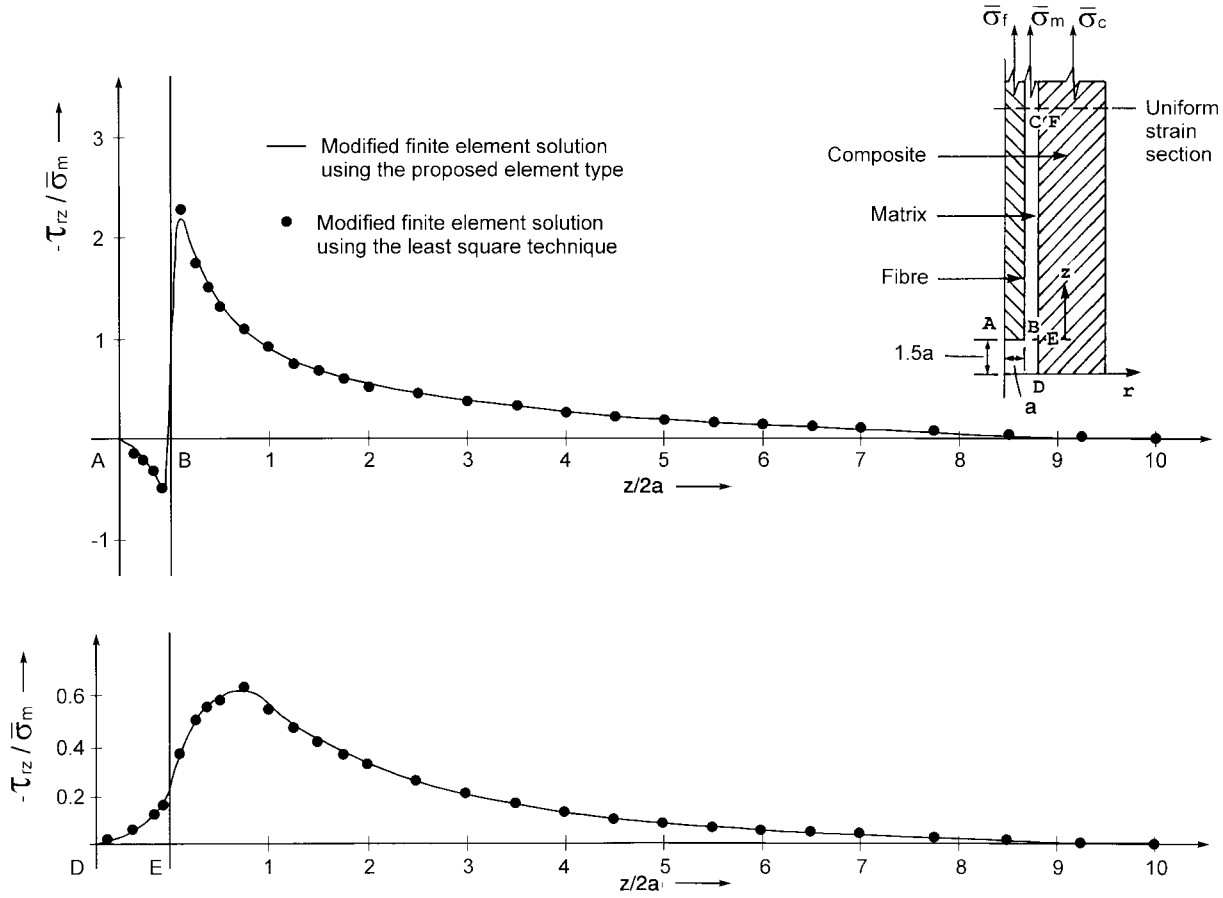

Fig. 12. Comparison of the interfacial shear stress distributions along the interfaces A–B–C and D–E–F obtained by the proposed element type and the least square technique.

very well in terms of both the shape and magnitude. This shows that the results obtained by the twenty-noded tri-material elements are not less accurate as compared with those of the twenty-noded bi-material elements. Thus, there is no necessity to increase the number of nodes significantly when the number of material types involved is increased.

7. Conclusions

The reliability and potential accuracy of the proposed multi-material element type for determining the stress distributions at the interfaces between different materials have been clearly illustrated. The improvement made by the use of the said element type is entirely due to the imposition of the necessary and sufficient equilibrium and compatibility conditions at the interface between different materials. It is worth noting that although the modified analysis procedure can provide comparable accuracy in determining the stress distributions at interfaces, the tedious procedure of least square fitting can be avoided by employing the proposed multi-material element type. Note that although the proposed element type is developed for accurate calculation of interfacial stresses, it can also be used to determine

the effective properties of composite materials similar to the model proposed by Alexander and Tzeng (1997). However, their model is much more versatile for determining the said properties.

The proposed approach for modifying finite elements is not confined to three-dimensional brick elements, but is equally applicable to all other element configurations with only minor or no modifications to the proposed approach.

Acknowledgements

This study was supported by the CRCG-fund of the University of Hong Kong.

References

Alexander, A., Tzeng, J.T., 1997. Three dimensional effective properties of composite materials for finite element applications. Journal of Composite Materials 31 (5), 466–485.

Bathe, K.J., 1996. Formulation and calculation of isoparametric finite element matrices. In: Finite Element Procedures. Prentice–Hall, Englewood Cliffs, New Jersey, pp. 338–484.

Buragohain, D.N., Ravichandran, P.K., 1994. Modified three-dimensional finite element for general and composite shells. Computers & Structures 51 (3), 289–298.

Librescu, L., Khdeir, A.A., 1988. Analysis of symmetric cross-ply laminated elastic plates using a higher-order theory: Part I — stress and displacement. Composite Structures 9, 189–213.

Murakami, H., 1986. Laminated composite plate theory with improved in-plane responses. Journal of Applied Mechanics 53, 661–666.

Noor, A.K., Burton, W.S., 1990. Assessment of computational models for multilayered anisotropic plates. Composite Structures 14, 233–265.

Reddy, J.N., 1989. On refined computational models of composite laminates. International Journal for Numerical Methods in Engineering 27, 361–382.

Di Sciuva, M., 1995. A third-order triangular multilayered plate finite element with continuous interlaminar stresses. International Journal for Numerical Methods in Engineering 38, 1–26.

Soh, A.K., 1993a. Improved method for determining interfacial stresses in composites. Journal of Aerospace Engineering 6 (1), 90–103.

Soh, A.K., 1993b. Determination of the mechanical properties of a composite using the least square method. Journal of Applied Mathematical Modelling 17 (5), 271–278.

Zienkiewicz, O.C., Taylor, R.L., 1989. Three-dimensional stress analysis. In: Basic Formulation and Linear Problems, The Finite Element Method, 4th, vol. 1. McGraw–Hill, UK, pp. 89–102.